

Analysis of Improved Particle Swarm Algorithm in Wireless Sensor Network Localization

Yafeng Chen

Department of Computer and Art Design, Henan Light Industry Vocational College, Zhengzhou, 450000, China

Abstract

WSN localization occupies an important position in the practical application of WSN. To complete WSN localization efficiently and accurately, the article constructs the objective function based on the target node location constraints and the maximum likelihood function. It avoids premature convergence through the PSO algorithm based on chaos search and backward learning. Based on linear fitting, the node-flipping fuzzy detection method is proposed to perform the judgment of node flipping fuzzy phenomenon. And the detection method is combined with the localization algorithm, and the final WSN localization algorithm is obtained after multi-threshold processing. After analysis, it is found that compared with other PSO algorithms, the MTLFPSO algorithm used in the paper has better performance with the highest accuracy of 83.1%. Different threshold values will affect the favorable and error detection rates of different WSNs. For type 1 WSNs, the positive detection rate of the 3-node network is the highest under the same threshold value, followed by the 4-node network; when the threshold value is 7.5 (3^E), the positive detection rate of the 3-node network is 97.8%. Different numbers of anchor nodes and communication radius will have specific effects on the number of definable nodes and relative localization error, in which the lowest relative localization error of the MTLFPSO algorithm is 3.4% under different numbers of anchor nodes; the lowest relative localization error of MTLFPSO algorithm is 2.5% under different communication radius. The article adopts the method to achieve accurate and efficient localization of WSNs.

Keywords: Improved particle swarm algorithm, WSN, Backward learning, Chaotic search, Linear fitting

Received on 09 June 2023, accepted on 24 August 2023, published on 11 September 2023

Copyright © 2023 Chen., licensed to EAI. This is an open access article distributed under the terms of the [CC BY-NC-SA 4.0](https://creativecommons.org/licenses/by-nc-sa/4.0/), which permits copying, redistributing, remixing, transformation, and building upon the material in any medium so long as the original work is properly cited.

doi: 10.4108/ew.3431

¹Corresponding author. Email: Yafeng_Chen2023@outlook.com

1. Introduction

With the continuous improvement of network technology, human interaction has changed significantly, in which Wireless Sensor Network (WSN) plays a significant role [1]-[3]. WSN can collect and process data information, such as the environment of the monitored area, in real time and deliver the processed information to the relevant users. In the process of information delivery, it is often necessary to know the location of the node where it is located to analyse the relevant information further. Therefore, the location of WSN nodes is a relatively important aspect. From the research contents of domestic and foreign scholars, it can be seen that there are more methods for WSN localization, such as genetic algorithm, Particle Swarm Optimization (PSO),

etc. Compared with the genetic algorithm, the PSO algorithm has a more significant advantage, which contains fewer parameters, is less challenging to implement, and has high localization accuracy [4]. Some scholars choose the PSO algorithm for optimal path selection of base stations based on multipath adaptive balanced routing to perform proportional allocation of system resources. The results show that the algorithm is better applied and can find the optimal path effectively [5]. According to the advantages of the PSO algorithm in the localization algorithm, the article uses the algorithm for the WSN node localization to effectively improve the localization accuracy.

2. Related work

WSNs belong to the distributed networks, which are more robust and have a low power consumption level, and have greater superiority, making their application in a wide range of applications, such as agriculture, industry, etc. In practical applications, the acquisition of node locations, is an important prerequisite for application implementation. Mann et al. faced with the problem of efficient clustering of WSNs, optimized the artificial swarm metaheuristic algorithm as a way to improve the utilization of the method. By improving the swarm sampling method, the method is made more efficient. Energy efficient clustering protocol is used to improve the energy efficiency of WSN. After simulation, it is found that the application of using the method is better [6]. Jj et al. provide a detailed analysis of the literature on location privacy protection of WSNs, an analytical summary of three model situations such as network models, a detailed analysis of the literature on location privacy protection of source nodes, aggregation nodes and three major classes of nodes containing both, and a comparison of the relevant performance, based on the literature review, pointing out the related issues and directions for further research [7]. Lu et al. used the WSN node scheduling and target localization evaluation method based on rotating nodes to perform multiple moving target tracking, and evaluated the related effects by network performance evaluation metrics. The results show that the use of the method is able to track targets effectively and has a balancing effect on node energy consumption [8]. Raja et al. proposed two solutions for multi-asset scenarios in order to be able to protect the source location privacy in WSNs and reduce the impact of random walk related methods. After comparing the performance of the related solutions, it is known that the use of the solution can better protect the location privacy [9]. Varshovi et al. address the problem of high volume of multimedia data in Wireless Multimedia Sensor Network (WMSN) by using the related processor for local image processing as a way to perform certain motion detection and send its related information to the base station. The results show the effectiveness of the detection method. The results show that the detection effect using the method is better [10].

Yu et al. In order to improve the stability of irregular tooth end mills, the radial cross section was designed parametrically, and the center coordinates of the end mill shape were calculated with the corresponding constructed mathematical model, and the spiral groove shape was optimized with the PSO algorithm. The results show that the accuracy of the mathematical model calculation is high and the optimization performance of the PSO algorithm is good, which improves the damping effect of the end mill.[11]. Purushothaman et al. solve the multi-objective problem existing in 5G networks by using the multi-objective self-organizing PSO algorithm to solve the multi-objective function of 5G wireless networks using large-scale multiplexed input-output techniques. The results show a good application of the method [12]. Diaz-Ramirez et al. address the problems of existing single-strain estimation

methods by using an iterative approach to optimize the single-point correspondence search by the PSO algorithm and perform operations such as template matching to perform single-strain parameter estimation. The comparison of the results shows that the estimation accuracy of the PSO algorithm is higher compared to other methods, and the use of the method can be applied effectively [13]. Bacar et al. solved the multi-objective vehicle path existence problem by using a multi-objective discrete PSO algorithm. The algorithm incorporates a variety of methods and after testing and analysis, the algorithm can effectively solve the problem of vehicle path existence [14]. Jubair et al. chose the social class-multi-objective PSO algorithm to solve, its existence of multi-objective optimization and variable length problems in a 2D environment, in the face of the problems of WSN deployment. The algorithm makes WSN deployment exist dynamic by fusing intra-class and inter-class operators. An application analysis of the used methods reveals that the improved PSO algorithm has a higher problem-solving capability [15].

In summary, in the field of WSN research, most of the research is on node location privacy protection, and there is little content on how to perform WSN localization. Therefore, the article takes WSN localization as the research object for further exploration. During this period, considering the good performance of PSO algorithm in heuristic search methods, the article uses it as a research method for WSN localization research.

3. Improved PSO algorithm in wireless sensor network localization

3.1 Two-way chaos search-based localization algorithm

WSNs are more widespread and have more applications. The node data information obtained on the basis of the known node location has important application value [16-18]. Not only that, the node location will have an important impact on the implementation of WSN load balancing and other aspects. Therefore, it is important to perform WSN node location. In WSN, the signal propagation model is shown in Equation (1).

$$RSS(d) = P_0 - 10\eta * \log_{10} d/d_0 + X \quad (1)$$

In Equation (1), the true and measured distances from the transmitting source to the receiving source are set to d and d_m , respectively, d_0 denotes the reference distance, P_0 denotes the energy received at d_0 , the Gaussian noise caused by the environment is set to X , and the path consumption index is η . And d_m can be expressed as Equation (2).

$$d_m = d_0 * 10^{\frac{P_0 - RSS(d)}{10\eta}} \quad (2)$$

Substituting Eq. (1) into Eq. (2), plus the fact that $10^{\frac{-x}{10\eta}}$ is very small and viewing $10^{\frac{-x}{10\eta}}$ approximately as a Gaussian variable with a mean of 1, gives Eq. (3).

$$d_m/d \sim N(1, \delta^2) \quad (3)$$

In Equation (3), N denotes the number of nodes and δ denotes the parameters. The distance measurement error will affect the positioning accuracy, and the node distance measurement value obeys Gaussian distribution, and the re-derivation of the positioning objective function is carried out. It sets the measured distance between nodes i and j as d_{mij} , d_{mij} probability distribution function can be obtained in Equation (4).

$$p(d_{mij}) = \frac{1}{\sqrt{2\pi(x_i - x_j)^2 + (y_i - y_j)^2} \sigma} e^{-\frac{\left(\frac{\sqrt{(x_i - x_j)^2 + (y_i - y_j)^2} - d_{mij}}{2\sigma^2}\right)^2}{2\sigma^2}} \quad (4)$$

Equation (4), $p(d_{mij})$ indicates the probability distribution function, i, j the true coordinate positions of $\langle x_i, y_i \rangle, \langle x_j, y_j \rangle$, e indicates the base of the natural logarithm.

Assuming the existence of N anchor nodes in the communication range of WSN target nodes, the maximum likelihood function of the relevant parameters can be known, after taking the logarithm of the function on both sides, so as to obtain the function in Equation (5).

$$f(x, y, \sigma) = \min_{x, y, \sigma} \sum_{i=1}^N \left(-\ln \frac{1}{\sqrt{2\pi(x_i - x)^2 + (y_i - y)^2} \sigma} + \frac{\left(\frac{\sqrt{(x_i - x)^2 + (y_i - y)^2} - d_m}{2\sigma^2}\right)^2}{2\sigma^2} \right) \quad (5)$$

In Equation (5), $f(x, y, \sigma)$ denotes the function. To carry out the node location constraints set, in WSN, it sets the node communication radius to R , if any target node Q can be directly received by the packet sent by the anchor node I, I can be referred to as Q's SingleBeacon, denoted by SBeacon; Conversely, if it cannot be directly received, it needs to rely on its single pick node in order to receive, I will be referred to as Q's DoubleBeacon set, denoted by DBeacon. Figure 1 shows the distribution of target nodes A and B with anchor nodes M and N.

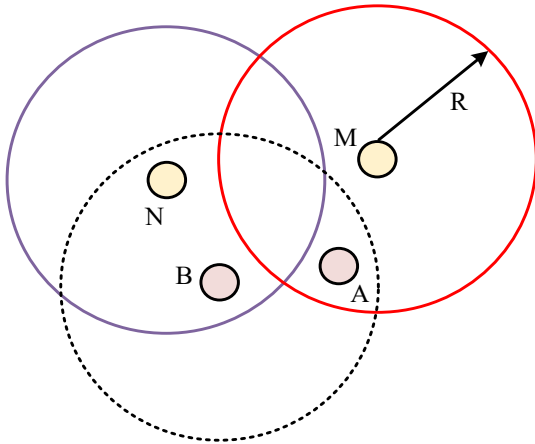


Fig 1. Node distribution diagram

In Figure 1, A is in the communication range of M, which means that M is the SBeacon of A; and A needs to receive information from N through B, which means that N is the DBeacon of A. The mathematical expression of A's position can be obtained in Equation (6).

$$\begin{cases} \text{dist}(A, B) \leq R, \forall B \in \text{SBeacon} \\ \text{dist}(A, B) > R, \forall B \in \text{DBeacon} \end{cases} \quad (6)$$

In Equation (6), $\text{dist}(A, B)$ is the Euclidean distance between A and B. For the target node A, its localization model is defined as Equation (5). On the basis of Equation (6), the constraints of the target node are obtained in Equation (7).

$$\begin{cases} \sqrt{(x_i - x)^2 + (y_i - y)^2} \leq R, B(x_i, y_i) \in \text{SBeacon} \\ \sqrt{(x_i - x)^2 + (y_i - y)^2} > R, B(x_i, y_i) \in \text{DBeacon} \end{cases} \quad (7)$$

On the basis of Eq. (7) and Eq. (5), the new objective function can be obtained by using the penalty function method as shown in Eq. (8).

$$h(x, y, \sigma) = f(x, y, \sigma) + \begin{cases} M[\max(0, \sqrt{(x_i - x)^2 + (y_i - y)^2} - R)], B(x_i, y_i) \in SBeacon \\ M[\max(0, R - \sqrt{(x_i - x)^2 + (y_i - y)^2})], B(x_i, y_i) \in DBeacon \end{cases} \quad (8)$$

In Equation (8), $h(x, y, \sigma)$ denotes the new objective function and M denotes the penalty factor. For WSN network localization, the article uses the PSO algorithm, which is faster in search, easy to implement, and has fewer parameters; Its algorithm flow chart is shown in Figure 2.

Fig 2. PSO algorithm process

In Fig. 2, there are five main steps, firstly, initialize the particle velocity and position in the population and determine the relevant parameters; calculate the fitness value; update the particle local extremes and the population global extremes; update the particle velocity and position, perform the check of the termination condition, if the number of population iterations is less than the threshold, revert to the step of calculating the fitness value and vice versa to terminate the iteration. output the optimal solution. Since the PSO algorithm is prone to fall into local optimum and early convergence problem, in order to be able to solve this problem, the article improves the PSO algorithm by introducing two strategies of elite learning and chaos search, so as to obtain a two-way chaos search-based localization algorithm, and its related process is shown in Figure 3.

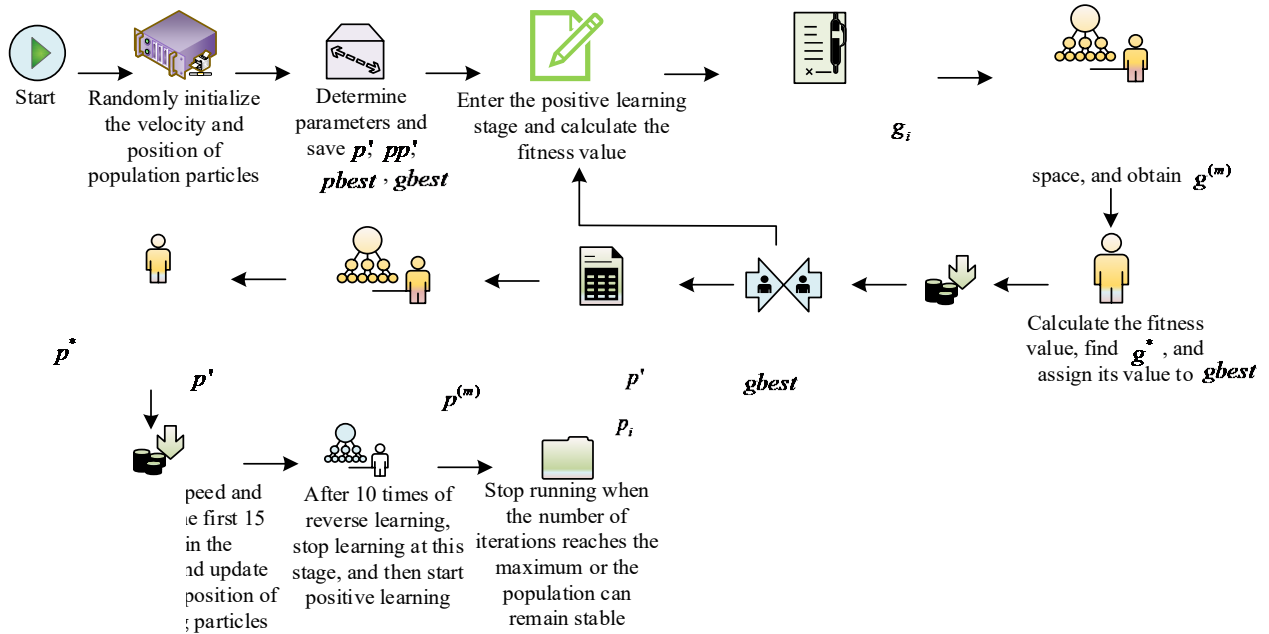
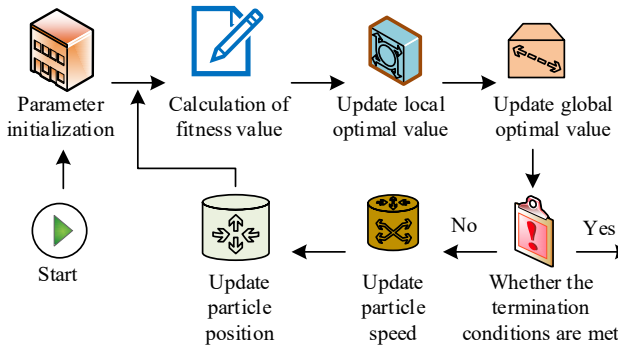


Fig 3. Improve PSO algorithm process

In Fig. 3, firstly, random initialization of population particle velocities and their positions are performed, and relevant parameters such as M , the number of populations n , and inertia weight coefficients ω are determined. The population worst solution p' and optimal solution $gbest$, and individual history worst solution pp' and optimal solution

$pbest$ are saved. Equation (8) is set into the population fitness function for forward learning. This stage can be divided into three parts, firstly, the value of particle fitness function is calculated if, then $f(x) < f(pbest)$ $pbest = X$; if, then $f(x) > f(pp')$ $pp' = X$; if $f(pbest) > f(gbest)$, then $gbest = pbest$; if $f(pp') > f(p')$, then $p' = pp'$.

Set the optimal position as $g^{best} = (g_1, \dots, g_N)$ and g_i as the element in g^{best} . It performs a chaotic search on it. The mapping of g_i to the domain of the definition of the chaos model^[0,1] is done by equation (9).

$$z_i = \frac{g_i - a_i}{b_i - a_i} \quad (9)$$

In Equation (9), z_i denotes the time parameter, and a_i and b_i denote the set elements. By iterating the chaotic model, a sequence of chaotic variables is generated at $z_i^{(m)}, m = (1, 2, \dots, h-1, h)$. Equation (10) reduces $z_i^{(m)}$ to

$$v_{id}^{k+1} = \omega * v_{id}^k + c_1 * r_1 * (pbest_{id}^k - x_{id}^k) + c_2 * r_2 * (gbest_d^k - x_{id}^k) \quad (11)$$

$$x_{id}^{k+1} = x_{id}^k + v_{id}^{k+1} \quad (12)$$

Equation (11), c_1, c_2 are learning factors, acceleration factors; c_1, c_2 are normal numbers, $c_1 = c_2 = 2$, r_1, r_2 are random numbers, they are uniformly distributed between 0-1, through ω can be the effect of particle flight speed on the population state, v indicates the particle speed; x indicates the particle position, k, d indicates the serial number. After 10 consecutive times, if the value of g^{best} remains unchanged, the corresponding population enters the reverse learning phase, and vice versa, it re-enters the forward learning phase. After entering the reverse learning phase, the phase can be divided into three parts. Firstly, the worst position is set as $P^1 = (p_1, \dots, p_N)$, and a chaos search is performed on P^1 , which is mapped to the definition domain of the chaos model^[0,1] through Equation (9) for P^1 . By iterating through the chaos model, a sequence of chaotic variables is generated $z_i^{(m)}, m = (1, 2, \dots)$. By reducing $z_i^{(m)}$ to the original solution space through Eq. (10), $P^{(m)} = (p_1^m, p_2^m, \dots, p_N^m)$ can be obtained. In the original search space, the fitness of each $P^{(m)}$ is calculated; Based on the calculated fitness, the worse solution P^* is found, and the value of this better solution is assigned to P^1 . In the first 15 particles of the population, the velocity and position of these particles are updated by Eqs. (11) and (12). In the update process of these particles, the individual historical worst solution and the population worst solution are pp^1 and P^1 , respectively. The velocities and positions of

the original solution space and obtains. $g^{(m)} = (g_1^m, g_2^m, \dots, g_N^m)$

$$g_i^m = a_i + b_i - a_i * z_i^m \quad (10)$$

In equation (10), $a_i < g_i < b_i$. In the original search space, the fitness of each $g^{(m)}$ is calculated; Based on the calculated fitness, a more optimal solution g^* is found and the value of this more optimal solution is assigned to g^{best} . The particle velocity and position are updated by Eqs. (11) and (12), during which g^{best} and p^{best} are treated as individual historical optimal solutions and population optimal solutions.

the remaining particles in the population are updated, during which the individual historical optimal solution and the population optimal solution are p^{best} and g^{best} , respectively. After 10 iterations of backward learning, this phase of learning is stopped, and then forward learning is started. The operation is stopped when the number of iterations reaches the maximum, or when the population can remain stable. During the operation of the algorithm, after each target node is localized, it becomes a pseudo-anchor node and participates in the subsequent iterations of the computation to help other target nodes to localize.

3.2 PSO localization algorithm based on multi-threshold linear fitting

In the process of WSN localization, ranging error occurs, which is not only due to the general PSO algorithm prone to local fitting, but also due to the node position flip-flop blurring phenomenon. Therefore, in addition to improving of PSO algorithm, the article also needs to solve the problem of node location flip-flop ambiguity. In WSN, there exist several common node localization flip-flop ambiguity detection methods, such as the linear presence detection method. Influenced by the linear fitting in machine learning, the article proposes the node flip-flop ambiguity detection method based on this, which is categorized as the linear presence detection method. Linear fitting can be referred to as linear regression, in which a predictive model of the relationship between the independent and dependent variables is established by least squares in the analysis process. For a given new independent variable, this prediction model allows the solution of its corresponding observations, as a solution to the situation where the original observation data set does not have corresponding observations. Specifically, the process of fuzzy detection of node flipping based on linear fitting is shown in Figure 4.

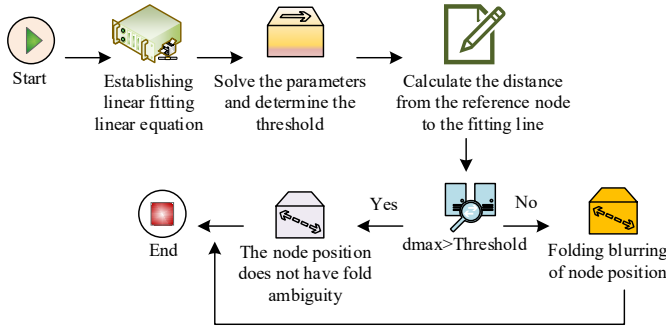


Fig 4. Fuzzy detection of node folding

In Figure 4, the position coordinates of the nodes are (x, y) , and the corresponding linear fitting equations are assumed to be shown in Equation (13).

$$a * x + b * y + c * z = 0 \quad (13)$$

In Equation (13), a, b, c are the parameters. The parameters a, b, c are solved, and the threshold value δ is determined. It calculates the distance between the reference point and the fitted line, set the maximum distance to d_{max} , and compare d_{max} with δ . If the maximum distance is less than the threshold value, it means that the target node is not flipped and blurred, otherwise, it means that the target node is flipped and blurred. The functions corresponding to a, b and c are set, and the corresponding mathematical expressions are shown in Equation (14).

$$f(a, b, c) = \min_{a, b, c} \sum_{i=1}^n \frac{|a * x_i + b * y_i + c|}{\sqrt{a^2 + b^2}} \quad (14)$$

In Equation (14), the position coordinates of the reference node are (x_i, y_i) . According to Eq. (14), the first-order derivatives of the parameters a, b , and c are carried out,

and the formula is simplified, and the relevant calculation formula is finally obtained as shown in Eq. (15).

$$\begin{cases} a * \bar{x} + b * \bar{y} + c = 0 \\ S_{xy} * a^2 - (S_{xx} - S_{yy}) * a * b - S_{xy} * b^2 = 0 \\ S_{xy} = \sum (x_i - \bar{x}) * (y_i - \bar{y}) \\ S_{xx} = (x_i - \bar{x})^2 \\ S_{yy} = (y_i - \bar{y})^2 \end{cases} \quad (15)$$

By using Eq. (15), the parameters a, b , and c can then be solved to obtain the values of the corresponding parameters. In node-position flipping fuzzy detection, the selection of the threshold value affects the positive detection rate of the detection method, which in turn affects the WSN localization accuracy. When the value of δ is set larger, the number of WSN locatable nodes decreases, thus making the WSN localization accuracy higher; Conversely, it makes more locatable points and the obtained localization accuracy decreases. Therefore, setting the threshold value reasonably can help to improve the localization accuracy of WSN. In this regard, the article carries out multi-threshold setting, and sets the threshold δ value to a larger value at the beginning of the node-flipping fuzzy detection method, which makes the number of locatable nodes of WSN appropriately less, thus improving the localization accuracy of WSN. Subsequently, in the iterative process, the threshold value of the previous iteration is decremented according to a fixed gradient $\Delta\delta$ at each iteration to obtain a sexual threshold value. Using the obtained new threshold, fuzzy flip detection and related localization operations are performed in the current iteration. When the localization is completed, the corresponding definable node is transformed into an anchor node and the rest of the nodes are left untouched. And with the decreasing threshold value, it makes the previously unlocatable nodes satisfy the fuzzy folding detection condition, which leads to an increase in the number of locatable nodes. The algorithm stops running when the termination condition is satisfied or the number of unlocatable nodes becomes 0. By combining the methods studied in the article, a PSO localization algorithm based on multi-threshold linear fitting is formed, and its flowchart is shown in Figure 5.

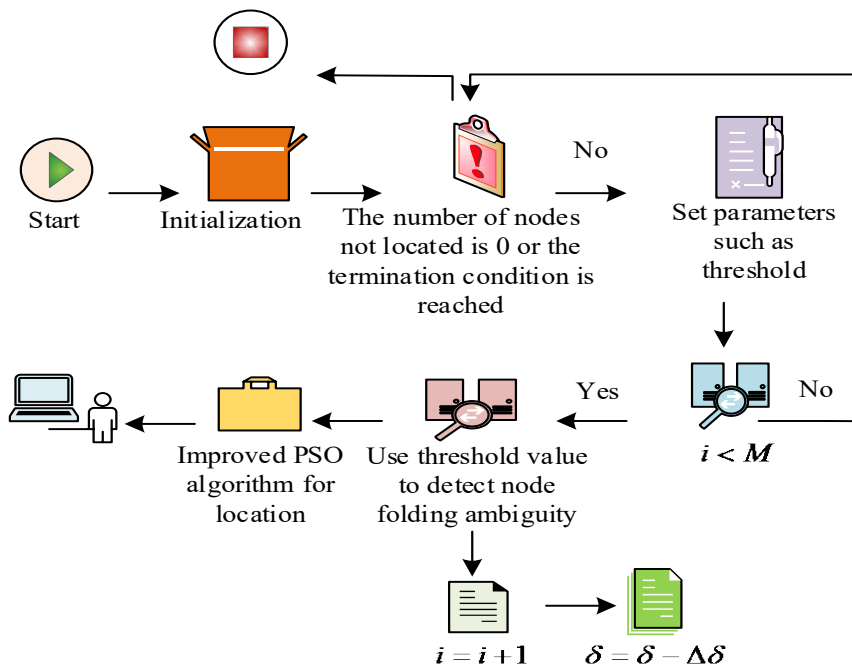


Fig 5. PSO location algorithm flow based on multi threshold linear fitting

In Fig. 5, after the initialization operation, the judgment of the number of unlocated nodes or the termination condition is performed. The algorithm is terminated when the number of unlocated nodes is 0 or the termination condition is satisfied, and the parameters such as threshold, fixed threshold and penalty factor are set on the contrary. When $i < M$, the threshold value is used to judge whether the node i is flipped and blurred; Otherwise, the judgment of the number of unlocated nodes or the termination condition is performed again. When a flip-flop blur occurs, $i = i + 1$, the threshold value of the previous iteration is subtracted from the fixed threshold value to obtain the new threshold value; conversely, the node is localized by the improved PSO-based localization algorithm, and after the completion of localization, the node is set as a pseudo-anchor node, $N = N + 1$, $i = i + 1$, the threshold value of the previous

iteration is subtracted from the fixed threshold value to obtain the new threshold value.

4. Analysis of multi-threshold linear fitting and PSO algorithm in WSN localization

In the article, the PSO localization algorithm based on multi-threshold linear fitting is set as MTLFPSO algorithm, and the PSO localization algorithm based on bidirectional chaos search is set as BCSPSO algorithm, and the general PSO algorithm and the BCSPSO algorithm are used as comparison algorithms to analyze the adaptation value, accuracy and recall of different algorithms under different iterations, as shown in Figure 6.

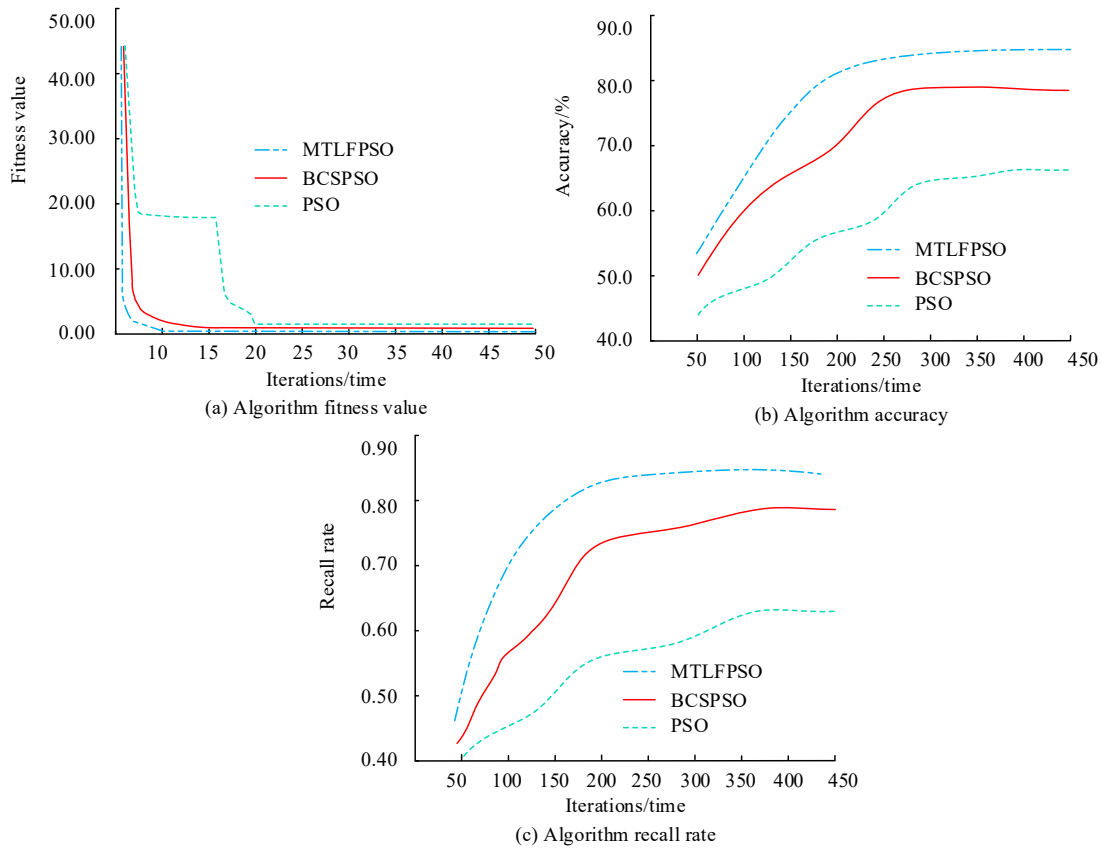


Fig 6. Performance comparison of different algorithms

In Fig. 6a, as the number of iterations increases, the adaptivity values of the three PSO algorithms decrease, while the curve where the MTLFPSO algorithm is located lies below the other algorithms and converges faster than the other algorithms. In Figure 6b, when the number of iterations is 250, the MTLFPSO algorithm has the highest accuracy of 83.1%, which is 5.7% higher than the BCSPSO algorithm, which has 77.4% accuracy, while the PSO algorithm has the lowest accuracy. In Figure 6c, the trend of the recall rate of the three algorithms is similar to the trend of the corresponding graph in Figure 6b, and overall, the MTLFPSO algorithm has the highest recall rate. This shows that the MTLFPSO algorithm has the best performance. The WSN type is divided into two types by using whether the node localization occurs flip-flop blur as the division criterion, setting the one that occurs flip-flop blur as type 1 and the one that does not occur flip-flop blur as type 2. The number of localization anchor nodes is used as the division criterion to divide the WSN type into three types, which are 3-node network, 4-node network, and 5-node network. Select 300 each of type 1 and type 2 networks, and the number of each type of network with all three node networks is 100. The variance is set to ε , and the network ranging error is set to the standard Gaussian distribution of $\varepsilon = 2.5$. The detection rates under different thresholds in different WSNs are investigated, and the results

are shown in Fig. 7.

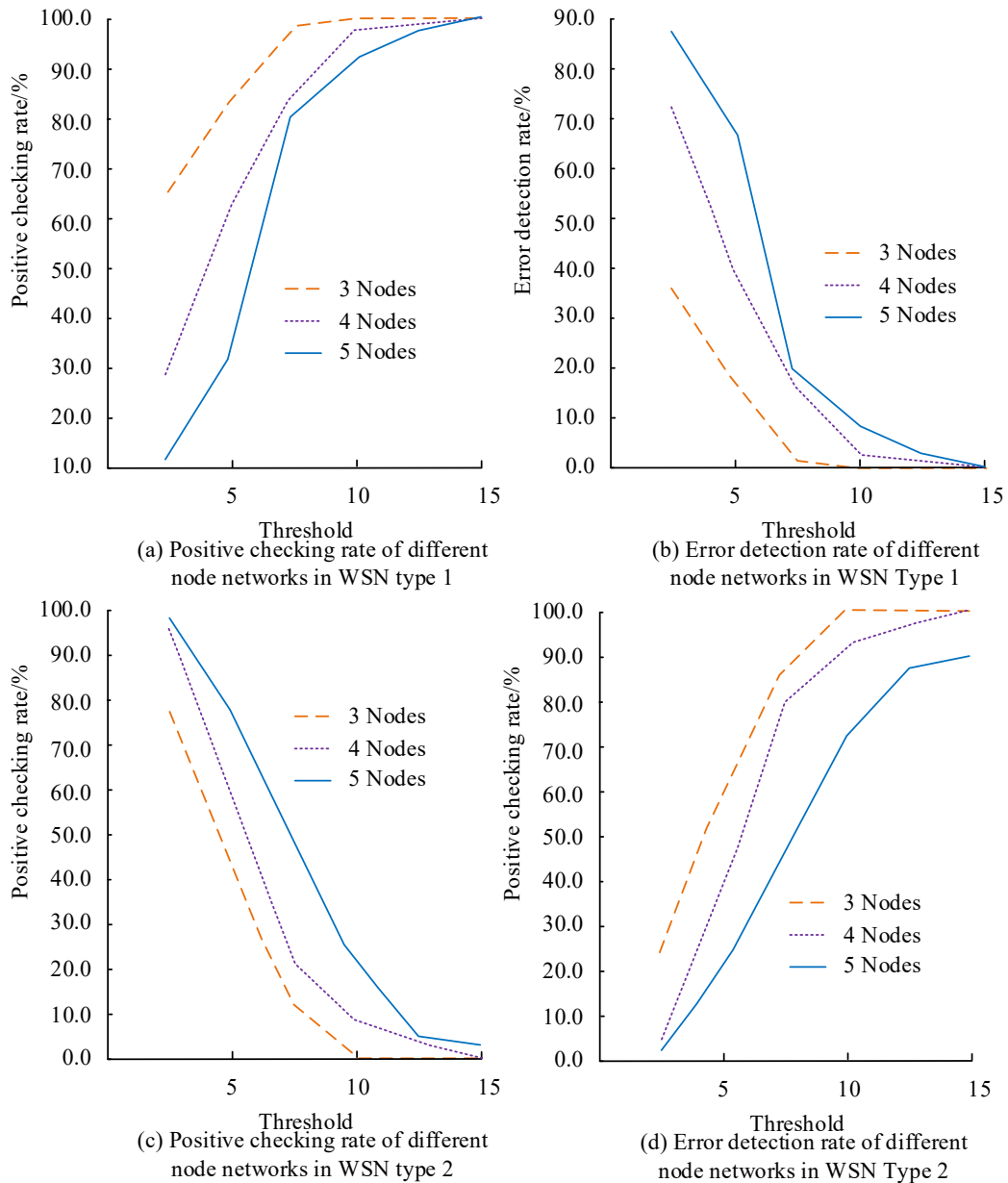
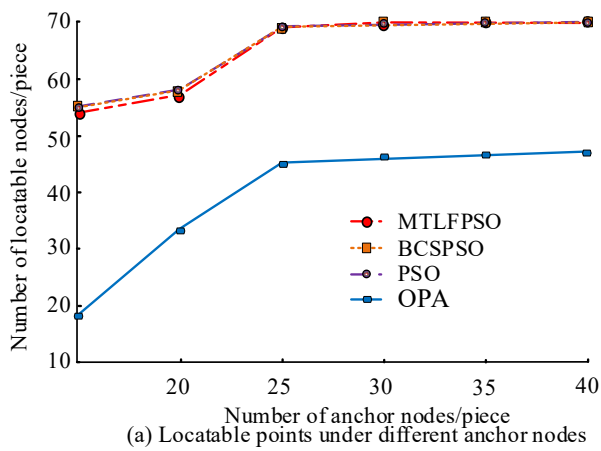


Fig 7. Detection rate under different thresholds in different WSNs

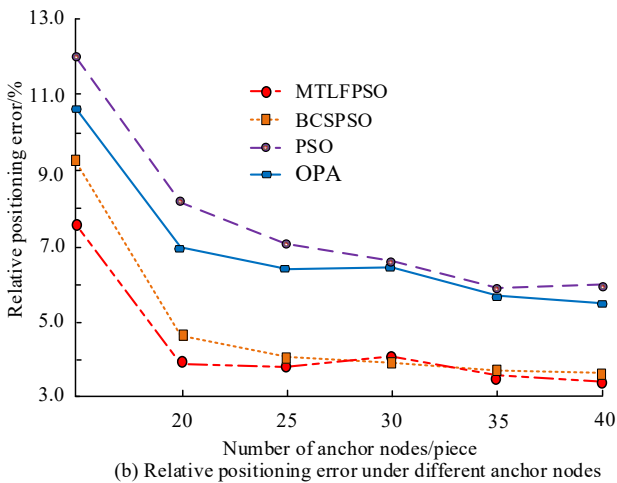
Figure 7a shows the positive detection rate of different node networks in type 1 WSN, Figure 7b shows the false detection rate of different node networks in type 1 WSN, Figure 7c shows the positive detection rate of different node networks in type 2 WSN, and Figure 6d shows the false detection rate of different node networks in type 2 WSN. In Fig. 7a, the positive detection rate of different node networks keeps increasing as the threshold value increases; the highest positive detection rate at the same threshold value is for the 3-node network, followed by the 4-node network. When the threshold value is 5, the positive detection rate of the 3-node network is 83.2%, which is 51.4% higher than that of the 5-node network, which is 31.8%; When the threshold value is 7.5 ($3^{\mathcal{E}}$), the positive detection rate of the 3-node network is 97.8%, which is significantly higher than 95.0%,

While the positive detection rate of the 4-node network is 84.7%, and the former is 13.1% higher than the latter. In Figure 7b, the error detection rate of the three node networks decreases continuously as the threshold value increases; Under the same threshold value, the error detection rate of the 3-node network is relatively low compared with the other two node networks. When the threshold value is 10, the error detection rate of the 3-node network is 0.0%, and the error detection rates of the 4-node network and the 5-node network are 2.1% and 6.4%, respectively. In Fig. 7c, the trend of the positive detection rate for different node networks is opposite to that in Fig. 6a, and the threshold value increases while the corresponding positive detection rate decreases continuously. When the threshold value is 2.5 (\mathcal{E}), the positive detection rates of all three node networks

are in the highest state, and the positive detection rates of the 4-node network and the 5-node network are 97.9% and 98.3%, respectively. In Fig. 7d, the trend of the false positive rate is opposite to that in Fig. 7b. When the threshold value is 10, the error detection rate of the 3-node network reaches 100.0%, which is higher than the other two node networks. Setting the node distribution area as 100×100 , the number of target nodes and anchor nodes as 70 and 30, respectively, the communication radius as 30, and the number of populations as 40, the node flipping fuzzy detection method based on orthogonal projection is set as the OPA algorithm, which is used as a comparison algorithm to study the number of locatable nodes and the relative localization error of different algorithms under different anchor node numbers as shown in Figure 8.



(a) Locatable points under different anchor nodes

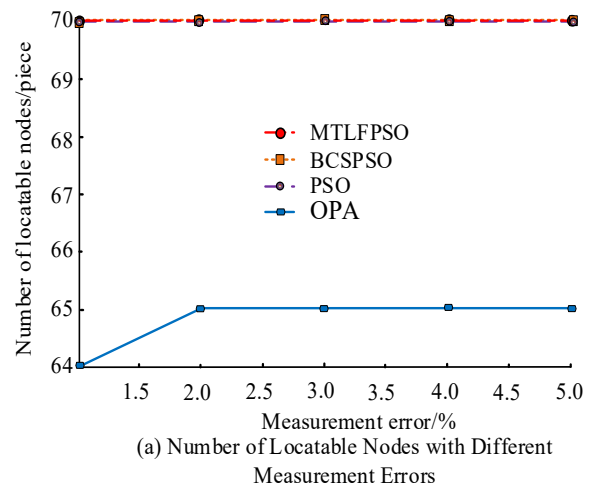


(b) Relative positioning error under different anchor nodes

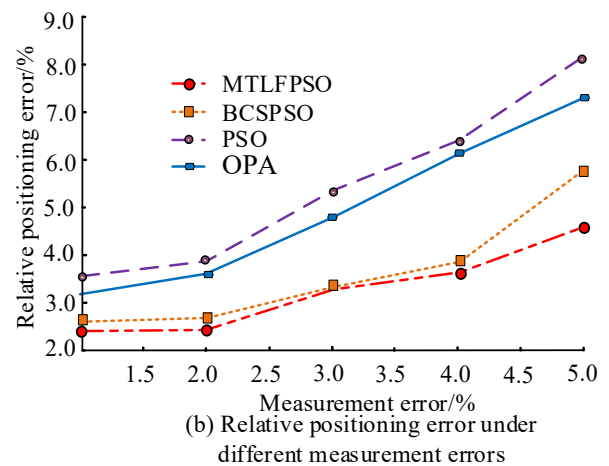
Fig 8. Number of locatable nodes and relative positioning error of different algorithms under different anchor nodes

In Figure 8a, as the number of anchor nodes increases, the number of locatable nodes of the three PSO algorithms first increases slowly and then increases more rapidly, and finally tends to be stable, and the three-fold lines overlap well; while the OPA algorithm first increases and then tends to be stable and lies below the fold lines of the three PSO

algorithms. When the number of anchor nodes is 25, the number of locatable nodes of the MTLFPSO algorithm is 68, which is the same as the other two PSO algorithms and 23 more than the OPA algorithm. The maximum number of locatable nodes of the MTLFPSO algorithm is 70, which is obviously more than that of the OPA algorithm. In Figure 8b, the relative positioning error of the four algorithms gradually decreases as the number of anchor nodes increases; with the same number of anchor nodes, the relative positioning error of the PSO algorithm is the largest, followed by the OPA algorithm, and the MTLFPSO algorithm has the lowest relative positioning error. When the number of anchor nodes is 40, the relative positioning error of the MTLFPSO algorithm is the lowest at 3.4%. The number of locatable nodes and relative positioning errors of these four algorithms under different measurement errors are analyzed in Figure 9.



(a) Number of Locatable Nodes with Different Measurement Errors



(b) Relative positioning error under different measurement errors

Fig 9. Number of locatable nodes and relative positioning error of different algorithms under different measurement errors

In Fig. 9a, as the measurement error increases, the number of locatable nodes of the three PSO algorithms remains the same, and the number of locatable nodes of the OPA

algorithm increases first and then remains the same. When the measurement error is 2.0%, the maximum number of locatable nodes of the OPA algorithm is 65, which is 5 less than that of the MTLFPSO algorithm. In Figure 9b, the relative localization error of the four algorithms gradually increases with the increase of the measurement error; the MTLFPSO algorithm has the lowest relative localization error under the number of measurement errors. When the measurement error is 5.0%, the relative localization error of the MTLFPSO algorithm is the highest at 4.1%. The number of locatable nodes and relative positioning errors of these four algorithms under different communication radii are studied in Figure 10.

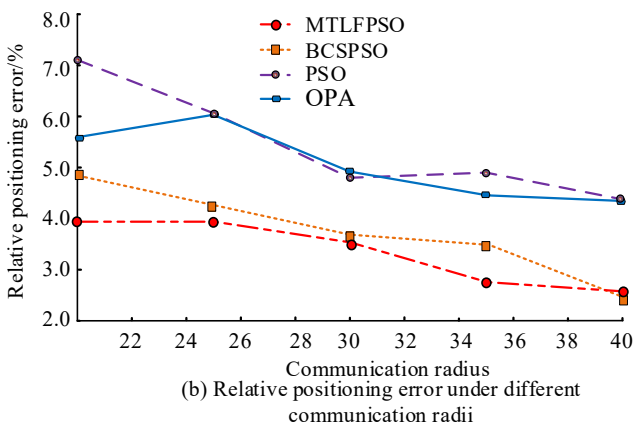
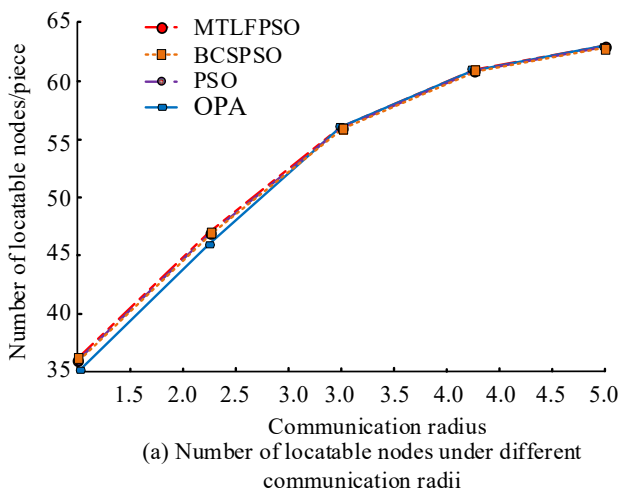


Fig 10. Number of locatable nodes and relative positioning error of different algorithms under different communication radii

In Fig. 10a, the number of locatable nodes of the four algorithms increases with the increase of the communication radius, and the number of locatable nodes of the algorithms is basically the same for the same communication radius. When the communication radius is 40, the maximum number of locatable nodes of the four algorithms is 63. In

Fig. 10b, as the increase of communication radius, the relative positioning error of the MTLFPSO algorithm and the OPA algorithm gradually decreases, while the relative positioning error of the BCSPSO algorithm and the PSO algorithm first decreases, then slightly increases, and then decreases again. When the communication radius is 40, the relative positioning error of the MTLFPSO algorithm is the lowest at 2.5%.

5. Conclusion

To be able to realize WSN localization, the article carries out the construction of network node localization models, selects the PSO algorithm as the localization algorithm, and carries out the algorithm optimization through chaotic search and backward learning to prevent the algorithm from falling into the optimal local situation. This optimization algorithm solves the problem of node flipping and blurring by multi-threshold linear fitting, thus forming a PSO localization algorithm based on multi-threshold linear fitting. The results show that compared with other PSO algorithms, the MTLFPSO algorithm used in the paper has better performance with the highest accuracy rate of 83.1%, which is 5.7% higher than the BCSPSO algorithm. Among different WSN detection rates, for type 1 WSN, the positive detection rate of the 3-node network is the highest under the same threshold value, followed by the 4-node network; When the threshold value is 7.5 (3^E), the positive detection rate of the 3-node network is 97.8%. For type 2 WSNs, the 3-node network has the relatively lowest error detection rate for the same threshold value. The maximum number of locatable nodes for the MTLFPSO algorithm is 70. Among the measurement errors, the MTLFPSO algorithm has the lowest relative localization error for the duplicate anchor nodes. When the measurement error is 5.0%, the highest relative positioning error of the MTLFPSO algorithm is 4.1%. Among different communication radii, when the communication radius is 40, the relative positioning error of the MTLFPSO algorithm is the lowest at 2.5%. This shows that the method used in the article has the highest localization accuracy, the lowest error, and high detection efficiency. In the future, the article can also explore the occurrence of flipping fuzzy node processing and test the accurate network algorithm to further improve the adaptability of the algorithm.

Fundings

The research is supported by: 2020 Training Plan for Young Key Teachers of Henan Higher Vocational Schools, Project Name: Research on Key Technologies of Dynamic Ideological Assessment of Vocational Students Based on Microblog, No.: 2020GZGG042; 2020 Henan Province Philosophy and Social Sciences Planning Project, project name: Research on the Construction of Teacher Ethics Evaluation System in Vocational Colleges in the New Era, No.: 2020BJY015.

References

- [1] Rajesh L, Mohan H S. Adaptive Group Teaching Based Clustering and Data Aggregation with Routing in Wireless Sensor Network. *Wireless personal communications: An International Journal*, 2022,122(2):1839-1866.
- [2] Dong C, Feng S, Yu F. Performance optimisation of multichannel MAC in large-scale wireless sensor network. *International Journal of Sensor Networks*, 2022, 38(1):12-24.
- [3] Dhinnesh A N, Sabapathi T. Probabilistic neural network based efficient bandwidth allocation in wireless sensor networks. *Journal of ambient intelligence and humanized computing*, 2022,13(4):2001-2012.
- [4] Jiang S, Mashdoor S, Parvin H, Bui Anh Tuan, Kim-Hung Pho. An Adaptive Location-Aware Swarm Intelligence Optimization Algorithm. *International Journal of Uncertainty, Fuzziness and Knowledge-Based Systems*, 2021,29(2): 249-279.
- [5] Sakthivel S, Manikandan M, Vivekanandhan V R. Design of efficient location-based multipath self-adaptive balancer router using particle swarm optimization in wireless sensor network. *International journal of communication systems*, 2022,35(4): e5060.1-e5060.14.
- [6] Mann P S, Singh S. Improved metaheuristic-based energy-efficient clustering protocol with optimal base station location in wireless sensor networks. *Soft Computing*, 2019, 23(3):1021-1037.
- [7] Jj A, Gh B, Hao W A, C MG. A survey on location privacy protection in Wireless Sensor Networks- ScienceDirect. *Journal of Network and Computer Applications*, 2019,125(Jan.):93-114.
- [8] Lu X, Zhang Y, Liu J, Yuan F, Cheng L. Mobile target tracking algorithm for wireless camera sensor networks with adjustable monitoring direction of nodes. *International Journal of Communication Systems*, 2019, 32(10): e3944.1-e3944.14.
- [9] Raja M, Koduru T, Datta R. Protecting Source Location Privacy in IoT Enabled Wireless Sensor Networks: The Case of Multiple Assets. *IEEE*, 2021,1(9):10807 - 10820.
- [10] Varshovi H, Kaviani Y S, Ansari-Asl K. Design and implementing wireless multimedia sensor network for movement detection using FPGA local co-processing. *Multimedia Tools and Applications*, 2019, 78(13):17413-17435.
- [11] Yu H, Zheng M, Zhang W, Nie W, Bian T. Optimal design of helical flute of irregular tooth end milling cutter based on particle swarm optimization algorithm. *Proceedings of the Institution of Mechanical Engineers, Part C. Journal of mechanical engineering science*, 2022,236(7):3323-3339.
- [12] Purushothaman K E, Nagarajan V. Multiobjective optimization based on selforganizing Particle Swarm Optimization algorithm for massive MIMO 5G wireless network. *International Journal of Communication Systems*, 2021,34(4): e4725.1-e4725.15.
- [13] Diaz-Ramirez V H, Juarez-Salazar R, Zheng J, Hernandez-Beltran JE, Marquez A. Homography estimation from a single-point correspondence using template matching and particle swarm optimization. *Applied optics*, 2022,61(7): D63-D74.
- [14] Bacar A, Rawhoudine S C. An attractors-based particle swarm optimization for multiobjective capacitated vehicle routing problem. *RAIRO - Operations Research*, 2021, 55(5):2599-2614.
- [15] Jubair A M, Hassan R, Aman A, Sallehudin H. Social class particle swarm optimization for variable-length Wireless Sensor Network Deployment. *Applied Soft Computing*, 2021,113(Pt.B):107926-1-107926-20.
- [16] Lin C, Han G, Qi X, J Du, T Xu, M Martinez-Garcia. Energy-Optimal Data Collection for Unmanned Aerial Vehicle-Aided Industrial Wireless Sensor Network-Based Agricultural Monitoring System: A Clustering Compressed Sampling Approach. *IEEE transactions on industrial informatics*, 2021,17(6):4411-4420.
- [17] Zali H M, Mahmood M, Pasya I, I Pasya, M Hirose, N Ramli. Narrowband and wideband EMW path loss in underwater wireless sensor network. *Sensor Review*, 2022,42(1):125-132.
- [18] Umashankar M L. An efficient hybrid model for cluster head selection to optimize wireless sensor network using simulated annealing algorithm. *Indian Journal of Science and Technology*, 2021, 14(3):270-288.